Altered subjective experience after psilocybin intake associates with a dynamic pattern of hyperconnected functional connectivity

Sepehr Mortaheb[1,2], Larry D. Fort[1,2], Natasha L. Mason[3], Pablo Mallaroni[3], Johannes G. Ramaekers[3*±], Athena Demertzi[1,2,4*±]

[±]Equal contribution

[1]Physiology of Cognition, GIGA-CRC In Vivo Imaging, University of Liège, Belgium

[2]Fund for Scientific Research FNRS, Brussels, Belgium

[3]Department of Neuropsychology and Psychopharmacology, Faculty of Psychology and Neuroscience, Maastricht University, The Netherlands

[4]Psychology & Neuroscience of Cognition (PsyNCog), University of Liège, Belgium

[*]Corresponding authors:

a.demertzi@uliege.be

j.ramaekers@maastrichtuniversity.nl

Abstract

To provide insights into the neurophenomenological richness after psilocybin intake, we investigated the link between brain dynamics and the ensuing alterations of reported experience. Healthy participants received either psilocybin (n=22) or placebo (n=27) while in ultra-high field 7T MRI scanning. Experiential changes were quantified using the 5-Dimensions of Altered States of Consciousness (5D-ASC) questionnaire, revealing alterations across all dimensions. Neuronally, psilocybin induced widespread increases in averaged functional connectivity. Time-varying analysis unveiled a recurrent hyperconnected pattern characterized by low BOLD signal amplitude, suggestive of heightened cortical arousal. Canonical correlation analysis linked the transition probabilities to this hyperconnected pattern with oceanic boundlessness and visionary restructuralization. We suggest that the brain's tendency to enter a hyperconnected-hyperarousal pattern under psilocybin may represent the potential to entertain variant mental associations in a creative way. For the first time these findings link brain dynamics with subjective alterations, providing new insights into the neurophenomenology of altered states of consciousness.

Introduction

Hallucinogens are psychoactive drugs that, historically, have been used to alter conscious experience[1,2]. These drugs are divided into the classes of serotonergic psychedelics (e.g., psilocybin), antiglutamatergic dissociatives (e.g., ketamine), anticholinergic deliriants (e.g., scopolamine) and kappa-opioid agonists (e.g., salvinorin A)[3]. Research on classical hallucinogens has focused largely on serotonergic psychedelics, such as lysergic acid diethylamide (LSD), ayahuasca, psilocybin, N-dimethyltryptamine (DMT), and mescaline[4]. Among them, psilocybin has been one of the most studied psychedelics, possibly due to its potential contribution to treating different disorders[5], such as obsessive-compulsive disorder[6], death-related anxiety[7], depression[8–11], treatment-resistant depression[12–14], major depressive disorder[15], terminal cancer-associated anxiety[11,16], demoralization[17], smoking [18], and alcohol and tobacco addiction[19–21].

Phenomenologically, the acute phase of psilocybin administration leads to the psychedelic state, which is the paradigmatic state of consciousness associated with consuming psilocybin and LSD[22]. The psychedelic state has been associated with the experience of ego dissolution (i.e., the reduction in self-referential awareness, ultimately disrupting self-world boundaries with increasing feelings of unity with others and own surroundings)[23,24], unconstrained and hyper-associative cognition[25,26], profound alterations in the perception of time, space and selfhood[27,28], perceptual alterations, synesthesia, amplification of emotional state[29], and emotional volatility[30]. Long-term and enduring effects have also been reported on personality and mood, such as increases in openness and extraversion, decreases in neuroticism, and increases in mindful awareness[31–33].

Regarding its neural effects, the administration of psilocybin acutely resulted in increased global connectivity with reduced modularity[34–36]. Region-wise, there were reports of decreased activity in the thalamus, posterior cingulate cortex, and medial prefrontal cortex[10], and altered connectivity of the claustrum[37]. Network-wise, decreased connectivity was reported within the default mode network (DMN)[1,10], visual network[1], and executive control network (ECN)[38], as well as reduced

segregation of dorsal attentional network and ECN[39]. These neural counterparts indicate that the subjective effects of psilocybin are linked to alterations in the activity and connectivity of important brain regions involved in information integration and routing when averaged signal analysis is concerned. Dynamic analyses of connectivity patterns after psilocybin administration have further shown that the brain tended to recurrently configure into transient functional states with low stability[40]. In addition, under psilocybin, there were higher probabilities for the brain to configure into a connectivity state characterized by a global cortex-wide positive phase coherence[41]. In terms of state transition dynamics, a recent study calculated the minimum network control energy required to transition between states (or maintain the same state) and found that the network control energy landscape was flattened under LSD and psilocybin, meaning that there were more frequent state transitions and increased entropy of brain pattern dynamics[42]. Taken together, averaged and dynamic connectivity analyses suggest that psilocybin alters brain function, such that it becomes functionally more connected, more fluid, and less modular.

What is of interest is that the link between the neuronal effects of psilocybin and the ensuing subjective alterations has been studied primarily in the context of averaged functional connectivity. Therefore, the question of how changes in the brain's functional connectome are linked with subjective alterations that individuals report remains unanswered. A recent investigation tried to correlate the occurrence rates of prominent connectivity patterns (i.e., frontoparietal subsystem and a globally coherent pattern) with subjective drug intensity (SDI) measured on a 10-point Likert scale[41,43]. Much as this approach has provided insights into the ensuing altered state of consciousness, it can be argued that, due to its simplicity, the SDI cannot capture the phenomenological richness of the psychedelic state. Here, we adopt a neurophenomenological approach after psilocybin intake in order to quantify its effects on cerebral functional dynamics and link these dynamic spatiotemporal fingerprints with reported experiential alterations measured with standardized tools.

Results

Data was collected from 49 healthy participants with previous experience with a psychedelic drug but not within the past three months[1]. Participants were allocated to two groups after being randomized to receive a single dose of psilocybin (0.17 mg/kg, n=22 (12 male, age=23±2.9 y) or placebo (bittering agent; n=27 (15 male, age=23.1±3.8 y). Six minutes of resting state with eyes open were acquired on fMRI ultra-high field 7T scanner during peak subjective drug effect (102 min post-treatment). The 5-Dimensional Altered States of Consciousness (5D-ASC) rating scale [24,44] was retrospectively evaluated at 360 min after drug administration.

Psilocybin administration leads to significant alterations in states of consciousness. Phenomenological outcome variables, including measures of the 5D-ASC and its 11-ASC factors (see Methods), were first assessed for normality assumptions. Shapiro-Wilk tests set at a significance level of 0.05 showed that all variables violated the assumption of normality (Table S1). As a result, Mann-Whitney U tests were used to compare the phenomenological outcomes in the two groups. Analyses revealed significant differences in all dimensions and factors with large effect sizes, such that the psilocybin group had more substantial effects than the placebo (Figure 1A and 1B, Table 1).

Functional connectivity and BOLD signal amplitude change after psilocybin administration. As a first step to investigate the neural effects of psilocybin, we estimated the average functional connectome of each subject over the acquisition time. We used the Schaefer atlas to parcellate the brain into 100 distinct regions of interest (ROI) and computed the Pearson correlations between pairs of ROIs. We found that after administration of psilocybin, whole-brain averaged connectivity increased (independent t-test: t=3.087, p=0.004; Figure 2A). This overall increase was further observed as a cortex-wide increase in the connectivity matrix values (independent t-test on the between-region connectivity values with FDR correction; Figure 2B). These alterations in the connectivity values were also accompanied by changes in the BOLD signal amplitude. By

calculating the Euclidean norm of the BOLD time series related to each ROI, we found that regional BOLD signal amplitude decreased after psilocybin administration in both posterior and anterior regions compared to the placebo group (independent t-test, FDR-corrected; Figure 2C, and Figure S1). While somatomotor, limbic network, and temporal regions of the DMN did not show significant changes in their signal norm, the highest decrease in BOLD signal amplitude was related to the posterior cingulate cortex and parietal regions of the ECN.

Next, we investigated the effect of psilocybin administration on the dynamic changes of the whole-brain functional connectome by estimating phase-based coherence connectivity matrices at each time point of the ROI time series. After concatenating all connectivity matrices across participants, we applied K-means clustering to summarize them into four connectivity patterns (Figure 2D). Variant and distinct profiles of complex inter-areal interactions emerged, including a pattern of both correlations and anti-correlations (Pattern 1), of anti-correlations of the DMN with other networks (Pattern 2), of global cortex-wide positive connectivity (Pattern 3), and of low inter-areal connectivity (Pattern 4). Pattern 3 occurred significantly more often in the psilocybin group when compared to the placebo group (independent t-test: t=3.731, p=0.001, $\alpha_{\text{bonferroni}} = 0.05/4 = 0.0125$, Figure 2D). Furthermore, using Markov modeling and considering each of the four patterns as model states, we estimated the transition probabilities of each state to the others. The psilocybin group showed significantly higher transition probabilities towards Pattern 3 from Pattern 1 (Wilcoxon Rank-Sum test: z=2.744, p=0.006), Pattern 3 (z=2.291, p=0.022), and Pattern 4 (z=2.000, p=0.045; Figure 2E). In addition, the psilocybin group showed lower transition probabilities from Pattern 2 to itself compared to the placebo group (z=-2.452, p=0.014).

The recurrent pattern of global hyperconnectivity is associated with experiences of oceanic boundlessness and visionary restructuralization. To investigate the neurophenomenological counterpart of psilocybin intake, canonical correlation analysis (CCA) was performed between the 11-ASC factors and the pattern transition probabilities. CCA is a method of assessing the

relationship between two multivariate datasets by maximizing their shared correlation, while reducing the potential of type-I error[45]. For this purpose, we estimated the first canonical vector for both the behavioral and neural space that maximize the shared correlation between two spaces ($r=0.97$, $p<0.001$). Considering the neural space, the transition probabilities from Pattern 1 to Pattern 3 showed the highest correlation with the first canonical vector of the neural space ($r=0.86$, $p<0.001$, Figure 3A). Transitions from Pattern 2 to Pattern 1 ($r=0.47$, $p=0.015$) and from Pattern 4 to Pattern 3 ($r=0.40$, $p=0.048$) showed lower significant correlations with the first canonical vector of the neural space. At the same time, in the phenomenological space, factors related to oceanic boundlessness (experience of unity: $r=0.80$, $p<0.001$, blissful state: $r=0.74$, $p<0.001$, insightfulness: $r=0.68$, $p<0.001$, spiritual experience: $r=0.62$, $p<0.001$, and disembodiment: $r=0.35$, $p=0.036$) and visionary restructuralization (elementary imagery: $r=0.67$, $p<0.001$, audio-video synesthesia: $r=0.61$, $p<0.001$, complex imagery: $r=0.50$, $p=0.001$, and changed meaning of percept: $r=0.50$, $p=0.001$) showed the highest correlations with the first canonical vector of the phenomenological space (Figure 3B). These observations show that the experiences of oceanic boundlessness and visual restructuralization after psilocybin administration are principally associated with the cerebral functional tendency to reconfigure into a global cortex-wide positive connectivity pattern.

Discussion

We investigated the effect of the serotonergic hallucinogen psilocybin on the brain's functional connectome with the aim to link them with alternations of conscious experience in order to better comprehend how the resulted neural and experiential changes are inter-connected. Overall, we found that psilocybin administration led to a tendency of the brain to recurrently configure in a globally hyperconnected pattern, which was linked to heightened reports about oceanic boundlessness (experience of unity, blissfulness, insightfulness, and spiritual experience), and visionary restructuralization (complex imagery, elementary imagery, audio-visual synesthesia, and changed meaning of percepts).

We first observed an overall increase in whole-brain functional connectivity in the psychedelic group, in line with previous reports[35,36]. Previous work showed that psychedelics, including psilocybin, changed the brain's functional organization into a new architecture, characterized by greater global integration, namely a higher amount of short-range and long-range functional connections[40,46]. That dynamic analysis showed that, under psilocybin, the brain had higher probabilities of transitioning to a hyperconnected pattern compared to the placebo group. Similar configurations and dynamic transitions have been reported by other studies with psychedelic drugs, as well[41]. This hyperconnected pattern is characterized by maximal integration and minimal segregation[47] and is interpreted as being functionally non-specific[41]. The significantly higher occurrence rate of this hyperconnected pattern in the psychedelic state can be explained by the "flattened landscape" theory[48]. Based on this theory, functionally specific connectivity states, which act as attractors in typical conditions, become less dominant under psychedelics, and, as such, the brain consumes less energy to transition between those states[42]. This reduction in the occurrence rate of functionally specific patterns, in turn, results in an increased transition probabilities to enter into the functionally non-specific hyperconnected pattern.

Moreover, we observed that this hyperconnected pattern is accompanied by cortex-wide decreases in the BOLD signal amplitude in the psychedelic group. As this amplitude reduction is cortex-wide, it leads to decreases in the global signal (GS) amplitude, which has been shown to act as an indirect measure of general arousal levels, namely higher GS amplitude is related to lower levels of arousal, and lower GS amplitudes is realated to higher levels of arousal[49–52]. Indeed, it was demonstrated that the GS amplitude correlated positively with relative amplitude of the delta band of EEG oscillations, and negatively with the relative amplitude of the alpha band[51]. Taken together, we conclude that the psychedelic state is realized by an overall high inter-areal integration, characterized by decreased GS amplitude, indicative of increased cortical arousal. More recently, we showed that when the hyperconnected pattern is accompanied by high GS amplitude during

wakeful rest, it is more probable that participants report phenomenological instances of mind blanking[53]. Mind blanking is the subjective evaluation of having no thoughts during unconstrained mentation[54], which was shown to be mediated by EEG slow-wave activity[55]. In that respect, the presence of a hyperconnected state suggests that regions co-vary together in the same way, and the GS amplitude is a complementary measure of the underlying neural activity.

The neurophenomenological analysis indicated that higher transition probabilities into the hyperconnected pattern are significantly associated with the factors of oceanic boundlessness. This altered state of consciousness is characterized by deeply-felt positive mood, feelings of insight, and experiences of unity[24]. Previous studies associated the positively experienced ego dissolution and oceanic boundlessness with reduced levels of hippocampal glutamate[1], and higher feelings of insight with reduced levels of DMN within-network static functional connectivity[26]. Our whole-brain dynamic analysis complements this literature by showing that the tendency of the brain to be recurrently hyperconnected after psilocybin intake can also explain the experiences of unity. This is important as this dimension is characterized by a disruption of self-world boundary[1] and the hyperconnected pattern is characterized by an atypical minimal segregation profile[47]. In fact, other studies showed that both integration and segregation are necessary for a coherent sense of self[56]. Moreover, we showed that this hyperconnectivity is also associated with the 5D-ASC dimension of visionary restructuralization, which refers to visual (pseudo)-hallucinations, illusions, auditory-visual synesthesia, and changes in the meaning of percepts after psilocybin administration[24]. Considering these two main findings, we postulate that the reported feelings of unity and visual pseudo-hallucinatory experiences under psilocybin being linked to the tendency of the brain to reside in a highly integrated state might represent the brain's potentiality to creatively entertain variant mental associations. This can be supported by the fact that different dimensions of creative thinking improve after psilocybin intake as a result of increased between-network functional

connectivity of DMN and frontoparietal network[26] which can also be achieved in the hyperconnected connectivity pattern.

This study is subject to various limitations. First, at the group level, the administration of psilocybin was not high enough to induce total ego dissolution for all participants. The administered dose was selected to be sufficient to induce a relevant psychedelic state that participants could endure in an ultra-high field scanner environment. However, our phenomenological analysis showed that this level of dose was adequate to achieve this purpose. Second, the lack of concurrent physiological recordings during fMRI scanning limits proper tracking of arousal level. In this study, we used the GS amplitude as a proxy to the level of cortical arousal. At the same time, the absence of simultaneous electrophysiological recordings limits the direct interpretation of neuronal firing during hyperconnected states. Simultaneous physiological and electrophysiological recordings in future studies can help to better investigate the role of arousal (cortical and general), and neuronal firing patterns in producing mystical experiences during the psychedelic state. Finally, the data-driven nature of the analysis can limit the results of the current study to the recruited population. However, this is less concerning in the dynamic functional connectivity analysis as in our previous studies it was shown that similar recurrent connectivity patterns can be derived in different datasets and different brain parcellations, showing their replicability and universality[47,53].

In conclusion, we found that pharmacological perturbations using psilocybin generate profound alterations both at the brain and at the experiential level. We showed that administration of psilocybin leads to an increase in the brain's tendency to configure into a functionally non-specific hyperconnected organization, which phenomenologically associates with experiences of oceanic boundlessness and visual pseudo-hallucinations. The present findings illuminate the intricate interplay between brain dynamics and subjective experience under psilocybin, providing new insights into the neurophenomenology of altered states of consciousness.

Methods

Participants. Data were collected from 49 healthy participants with previous experience with a psychedelic drug, but not within the past 3 months of the experiment. Participants were randomized to receive a single dose of psilocybin (0.17 mg/kg, n=22; 12 male; age=23±2.9 y) or placebo (n=27; 15 male; age=23.1±3.8 y). This study was conducted according to the code of ethics on human experimentation established by the declaration of Helsinki (1964) and amended in Fortaleza (Brazil, October 2013) and in accordance with the Medical Research Involving Human Subjects Act (WMO) and was approved by the Academic Hospital and University's Medical Ethics committee (Maastricht University, Netherlands Trial Register: NTR6505). All participants were fully informed of all procedures, possible adverse reactions, legal rights, responsibilities, expected benefits, and their right for voluntary termination without consequences.

Datasets. Six minutes of resting state fMRI were acquired from the participants with eyes open during peak subjective drug effect (102 minutes post-treatment). In addition, the Five Dimensions of Altered States of Consciousness (5D-ASC) questionnaire was administered 360 minutes after drug intake, as retrospective measures of drug effects.

Phenomenological Assessment. The 5D-ASC is a 94-item self-report scale that assesses the participants' alterations from normal waking consciousness[44]. In this questionnaire participants are asked to make a vertical mark on the 10-cm line below each statement to rate to what extent the statements applied to their experience in retrospect from "No, not more than usually" to "Yes, more than usually." The 5D-ASC comprises five dimensions, including *oceanic boundlessness* (OBN), *dread of ego dissolution* (DED), *visionary restructuralization* (VRS), auditory *alterations* (AUA), and *reduction of vigilance* (VIR). Further, OBN, DED, and VRS can be decomposed into 11 subscales via a previously published factor analysis[24]: OBN: *experience of unity*, *spiritual experience*, *blissful state*, *insightfulness*, *disembodiment*, DED: *impaired control and cognition*, *anxiety*, and VRS: *complex imagery*, *elementary imagery*, *audio-visual synesthesia*, and *changed meaning of percepts* constructing 11-ASC measurement system.

Imaging Setup. Images were acquired on a 7T Siemens Magnetom scanner (Siemens Medical, Erlangen, Germany) using 32 receiving channel head array Nova coil (NOVA Medical Inc., Wilmington MA). The T1w images were acquired using a magnetisation-prepared 2 rapid acquisition gradient-echo (MP2RAGE) sequence collecting 190 sagittal slices following parameters: repetition time (TR) = 4500 ms, echo time (TE) = 2.39 ms, inversion times TI1 /TI2 = 900/2750 ms, flip angle1 = 5°, flip angle2 = 3°, voxel size = 0.9 mm isotropic, bandwidth = 250 Hz/pixel. In addition, 258 whole-brain EPI volumes were acquired at rest (TR = 1400 ms; TE = 21 ms; field of view=198 mm; flip angle = 60°; oblique acquisition orientation; interleaved slice acquisition; 72 slices; slice thickness = 1.5 mm; voxel size = 1.5 × 1.5 × 1.5 mm).

Phenomenological Analysis. 5D-ASC and its 11-ASC factors were assessed for normality assumptions using Shapiro-Wilk tests. Due to violations in normality, non-parametric Mann-Whitney U tests were performed to compare the 5D-ASC and 11-ASC scores between two groups. P-values were corrected using Bonferroni method with a significance level of $\alpha = 0.05$. The effect size was calculated based on Glass rank biserial coefficient (rg).

Neuroimaging Data Preprocessing. FMRI data were preprocessed using locally developed pipeline based on SPM12[57]. After susceptibility distortion correction and realignment, functional data were registered to the high resolution T1 image, then normalized to the standard MNI space, and finally was smoothed using a Gaussian kernel with a full width at half maximum (FWHM) of 6mm. After segmentation of structural T1 image into grey matter (GM), white mater (WM), and CSF masks, the bias corrected structural image and all the extracted masks were normalized to the MNI space. Further, WM and CSF masks were eroded by one voxel to remove any overlapping between these tissues and the GM voxels. To denoise functional time series, we used a locally developed pipeline written in Python [nipype package[58]]. In this pipeline, a general linear model (GLM) was fitted to each voxel data separately, regressing out the effect of six movement parameters (translation in x, y, and z directions, and rotation in yaw, roll, and pitch directions) and

their first derivative, constant and linear trends using zero-order and first-order Legendre polynomials, 5 principal components of signals in the WM and CSF masks, and outlier data points. Outlier detection was performed using ART toolbox (http://web.mit.edu/swg/software.htm). Any volume with a movement value of greater than 3 mm, rotation value of greater than 0.05 radians, and z-normalized global signal intensity of greater than 3 was considered as an outlier. After regressing out these nuisance regressors, the remaining signal was filtered in the range of [0.008, 0.09] Hz and was used for further analysis. The Schaefer atlas with 100 ROIs and a resolution of 2mm[59] was used to extract the averaged BOLD signals inside each ROI.

Averaged Functional Connectivity. Pearson correlations were calculated between the BOLD time series of each pair of ROIs, Fisher transformed, and a 100×100 connectivity matrix was created for each participant. Independent t-test was used to compare the 4950 possible between-region connectivity values between two groups. FDR correction was performed to correct for multiple comparison. Further, the average of the connectivity values over the whole brain was calculated for each participant and was considered as the overall connectivity value of the brain. An independent t-test was performed to compare the overall connectivity values between psilocybin and placebo groups.

Time-varying Functional Connectivity. We used phase-based coherence analysis to extract between-region connectivity patterns at each time point of the scanning session[47,60]. For each participant i, after z-normalization of time series at each region r (i.e., $x_{i,r}[t]$), the instantaneous phase of each time series was calculated via Hilbert transform as:

$$\hat{x}_{i,r}(t) = \frac{1}{\pi t} * x_{i,r}(t)$$

where * indicates a convolution operator. Using this transformation, we produced an analytical signal for each regional time series as:

$$x_{i,r}^{a}(t) = x_{i,r}(t) + j\hat{x}_{i,r}(t)$$

where $j = \sqrt{-1}$. From this analytical signal, the instantaneous phase of each time series can be estimated as:

$$\varphi_{i,r}(t) = \tan^{-1}\left(\frac{\hat{x}_{i,r}(t)}{x_{i,r}(t)}\right)$$

After wrapping each instantaneous phase signal of $\varphi_{i,r}(t)$ to the $[-\pi, \pi]$ interval and naming the obtained signal as $\theta_{i,r}(t)$, we calculated a connectivity measure for each pair of regions as the cosine of their phase difference. For example, the connectivity measure between regions r and s in subject i was defined as:

$$conn_{i,r,s}(t) \triangleq \cos\left(\theta_{i,r}(t) - \theta_{i,s}(t)\right)$$

By this definition, completely synchronized time series lead to a connectivity value of 1, completely desynchronized time series produce a connectivity value of zero, and anticorrelated time series produce a connectivity measure of -1. Using this approach, we created a connectivity matrix of 100×100 at each time point t for each subject i that we called $C_i(t)$:

$$C_i(t) \triangleq \left[conn_{i,r,s}(t)\right]_{r,s}$$

After collecting the connectivity matrices across all time points and participants, k-means clustering was applied, with 500 repetitions and 200 iterations at each repetition. With this technique, four robust and reproducible patterns were extracted as the centroids of the clusters, and each resting connectivity matrix was assigned to one of the extracted patterns.

We calculated the occurrence rate of each pattern defined as the proportion of connectivity matrices assigned to that pattern and was calculated for each subject separately. Independent two-tailed t-tests were used to compare the occurrence rate of each FC pattern between the psychedelic and placebo group. Bonferroni correction was used to correct the p-values for multiple comparisons across the four connectivity patterns.

Dynamic state transition modeling. To investigate the temporal evolution of the identified connectivity matrices, we defined the extracted patterns as the distinct states of a dynamical system transitioning between them over time using Markov modelling[47]. Using this approach, the data of a sample participant could be stated as a sequence of connectivity patterns over time (i.e., $\{P_t \mid t: 1, \dots, T \; and \; P_t \in \{1, \dots, M\}\}$, where M is the number of patterns and T is the number of signal time points). In this case, the probability of transitioning from Pattern I to Pattern J defined as $p(I \rightarrow J)$, considering $I, J \in \{1, .., M\}$, can be calculated as the number of consecutive I, J pairs in the sequence, divided by the total number of transitions from pattern I:

$$p(I \rightarrow J) = \frac{\sum_{t=0}^{T-1}[(P_t == I) \,\&\, (P_{t+1} == J)]}{\sum_{j=1}^{M}\sum_{t=0}^{T-1}[(P_t == I) \,\&\, (P_{t+1} == j)]}$$

This transition probability was estimated for each possible between-state transition and each subject separately. With this approach, we could compare any significant difference in transition probabilities between two groups of subjects. To detect significantly different transition probabilities between the two groups, Wilcoxon rank-sum test was performed on each transition and p-values were FDR-corrected.

Regional BOLD Amplitude Analysis. The Euclidean norm of the BOLD signal was calculated at each ROI as a measure of the power of the signal. Independent t-test was used to compare the regional GS power between two groups and p-values were FDR-corrected due to multiple comparisons.

Neurophenomenological Analysis. A canonical correlation (CCA) analysis was conducted using the sixteen dynamic patterns transition probability variables as features of the neuronal space, and the 11-ASC and EDI variables as features of the phenomenological space, in order to evaluate the multivariate shared relationship between the two variable sets. CCA is a multivariate latent variable model that identifies associations between two different data modalities[45]. Considering matrix $X^{N \times M}$ contains M neuronal features of N subjects, and $Y^{N \times P}$ contains P phenomenological

features of N subjects, the objective of the CCA is to find pairs of neuronal and phenomenological weights $w_x^{M\times 1}$ and $w_y^{P\times 1}$ such that the weighted sum of the neuronal and phenomenological variables maximizes the correlation between the resulting latent variables (canonical variates):

$$\max_{w_x, w_y} corr(Xw_x, Yw_y)$$

After finding latent variables Xw_x and Yw_y that have the maximal correlation, the features in each modality of data that have a stronger correlation with their respective latent variable are also significantly associated with one another.

Data availability

The connectomes and the accompanying covariates used to differentiate individuals can be made available to qualified research institutions upon reasonable request to J.G.R. and a data use agreement executed with Maastricht University.

Code availability

All codes used for analysis are freely available at https://gitlab.uliege.be/S.Mortaheb/psychedelics

Author contributions

JR & AD contributed to the conception and design of the work; NM acquired the data; SM & LDF contributed with data analysis; all authors contributed to data interpretation; SM, LF, & AD drafted and revised the manuscript; all authors proofread the submitted work.

Acknowledgments

This article was supported by the Belgian Fund for Scientific Research (FRS-FNRS), the European Union's Horizon 2020 Research and Innovation Marie Skłodowska-Curie RISE programme NeuronsXnets (grant agreement 101007926), the European Cooperation in Science and Technology COST Action (CA18106), the Léon Fredericq Foundation, and the University and of University Hospital of Liège.

References

1. Mason, N. L. *et al.* Me, myself, bye: regional alterations in glutamate and the experience of ego dissolution with psilocybin. *Neuropsychopharmacol.* **45**, 2003–2011 (2020).
2. Metzner, R. Hallucinogenic Drugs and Plants in Psychotherapy and Shamanism. *Journal of Psychoactive Drugs* **30**, 333–341 (1998).
3. Volgin, A. D. *et al.* Understanding Central Nervous System Effects of Deliriant Hallucinogenic Drugs through Experimental Animal Models. *ACS Chem. Neurosci.* **10**, 143–154 (2019).
4. Nichols, D. E. Psychedelics. *Pharmacol Rev* **68**, 264–355 (2016).
5. Kwan, A. C., Olson, D. E., Preller, K. H. & Roth, B. L. The neural basis of psychedelic action. *Nat Neurosci* **25**, 1407–1419 (2022).
6. Moreno, et al. Safety, Tolerability, and Efficacy of Psilocybin in 9 Patients With Obsessive-Compulsive Disorder. (2006).
7. Grob, C. S. *et al.* Pilot Study of Psilocybin Treatment for Anxiety in Patients With Advanced-Stage Cancer. *Arch Gen Psychiatry* **68**, 71 (2011).
8. Andersen, K. A. A., Carhart-Harris, R., Nutt, D. J. & Erritzoe, D. Therapeutic effects of classic serotonergic psychedelics: A systematic review of modern-era clinical studies. *Acta Psychiatr. Scand.* **143**, 101–118 (2021).
9. Carhart-Harris, R. L. *et al.* Trial of Psilocybin versus Escitalopram for Depression. *N Engl J Med* **384**, 1402–1411 (2021).
10. Carhart-Harris, R. L. *et al.* Neural correlates of the psychedelic state as determined by fMRI studies with psilocybin. *Proc. Natl. Acad. Sci. U.S.A.* **109**, 2138–2143 (2012).
11. Ross, S. *et al.* Rapid and sustained symptom reduction following psilocybin treatment for anxiety and depression in patients with life-threatening cancer: a randomized controlled trial. *J Psychopharmacol* **30**, 1165–1180 (2016).
12. Carhart-Harris, R. L. *et al.* Psilocybin with psychological support for treatment-resistant depression: an open-label feasibility study. *The Lancet Psychiatry* **3**, 619–627 (2016).

13. Carhart-Harris, R. L. *et al.* Psilocybin for treatment-resistant depression: fMRI-measured brain mechanisms. *Sci Rep* **7**, 13187 (2017).

14. Carhart-Harris, R. L. *et al.* Psilocybin with psychological support for treatment-resistant depression: six-month follow-up. *Psychopharmacology* **235**, 399–408 (2018).

15. Davis, A. K. *et al.* Effects of Psilocybin-Assisted Therapy on Major Depressive Disorder: A Randomized Clinical Trial. *JAMA Psychiatry* **78**, 481 (2021).

16. Griffiths, R. R. *et al.* Psilocybin produces substantial and sustained decreases in depression and anxiety in patients with life-threatening cancer: A randomized double-blind trial. *J Psychopharmacol* **30**, 1181–1197 (2016).

17. Anderson, B. T. *et al.* Psilocybin-assisted group therapy for demoralized older long-term AIDS survivor men: An open-label safety and feasibility pilot study. *EClinicalMedicine* **27**, 100538 (2020).

18. Johnson, M. W., Garcia-Romeu, A. & Griffiths, R. R. Long-term follow-up of psilocybin-facilitated smoking cessation. *The American Journal of Drug and Alcohol Abuse* **43**, 55–60 (2017).

19. Bogenschutz, M. P. *et al.* Psilocybin-assisted treatment for alcohol dependence: A proof-of-concept study. *J Psychopharmacol* **29**, 289–299 (2015).

20. Garcia-Romeu, A. *et al.* Cessation and reduction in alcohol consumption and misuse after psychedelic use. *J Psychopharmacol* **33**, 1088–1101 (2019).

21. Johnson, M. W., Garcia-Romeu, A., Cosimano, M. P. & Griffiths, R. R. Pilot study of the 5-HT $_{2A}$ R agonist psilocybin in the treatment of tobacco addiction. *J Psychopharmacol* **28**, 983–992 (2014).

22. Bayne, T. & Carter, O. Dimensions of consciousness and the psychedelic state. *Neuroscience of Consciousness* **2018**, niy008 (2018).

23. Nour, M. M. & Carhart-Harris, R. L. Psychedelics and the science of self-experience. *Br J Psychiatry* **210**, 177–179 (2017).

24. Studerus, E., Gamma, A. & Vollenweider, F. X. Psychometric Evaluation of the Altered States of Consciousness Rating Scale (OAV). *PLoS ONE* **5**, e12412 (2010).

25. Girn, M., Mills, C., Roseman, L., Carhart-Harris, R. L. & Christoff, K. Updating the dynamic framework of thought: Creativity and psychedelics. *NeuroImage* **213**, 116726 (2020).

26. Mason, N. L. *et al.* Spontaneous and deliberate creative cognition during and after psilocybin exposure. *Transl Psychiatry* **11**, 209 (2021).

27. Carhart-Harris, R. L. *et al.* The entropic brain: a theory of conscious states informed by neuroimaging research with psychedelic drugs. *Front. Hum. Neurosci.* **8**, (2014).

28. Griffiths, R. R., Richards, W. A., McCann, U. & Jesse, R. Psilocybin can occasion mystical-type experiences having substantial and sustained personal meaning and spiritual significance. *Psychopharmacology* **187**, 268–283 (2006).

29. Preller, K. H. & Vollenweider, F. X. Phenomenology, structure, and dynamic of psychedelic states. *Behavioral neurobiology of psychedelic drugs* 221–256 (2018).

30. Majić, T., Schmidt, T. T. & Gallinat, J. Peak experiences and the afterglow phenomenon: When and how do therapeutic effects of hallucinogens depend on psychedelic experiences? *J Psychopharmacol* **29**, 241–253 (2015).

31. Erritzoe, D. *et al.* Effects of psilocybin therapy on personality structure. *Acta Psychiatr Scand* **138**, 368–378 (2018).

32. MacLean, K. A., Johnson, M. W. & Griffiths, R. R. Mystical experiences occasioned by the hallucinogen psilocybin lead to increases in the personality domain of openness. *J Psychopharmacol* **25**, 1453–1461 (2011).

33. Madsen, M. K. *et al.* A single psilocybin dose is associated with long-term increased mindfulness, preceded by a proportional change in neocortical 5-HT2A receptor binding. *European Neuropsychopharmacology* **33**, 71–80 (2020).

34. Daws, R. E. *et al.* Increased global integration in the brain after psilocybin therapy for depression. *Nat Med* **28**, 844–851 (2022).

35. Preller, K. H. *et al.* Psilocybin Induces Time-Dependent Changes in Global Functional Connectivity. *Biological Psychiatry* **88**, 197–207 (2020).

36. Roseman, L., Leech, R., Feilding, A., Nutt, D. J. & Carhart-Harris, R. L. The effects of psilocybin and MDMA on between-network resting state functional connectivity in healthy volunteers. *Front. Hum. Neurosci.* **8**, (2014).
37. Barrett, F. S., Krimmel, S. R., Griffiths, R. R., Seminowicz, D. A. & Mathur, B. N. Psilocybin acutely alters the functional connectivity of the claustrum with brain networks that support perception, memory, and attention. *NeuroImage* **218**, 116980 (2020).
38. McCulloch, D. E.-W., Madsen, M. K. & Stenb, D. S. Lasting effects of a single psilocybin dose on resting-state functional connectivity in healthy individuals. *Journal of Psychopharmacology* 11 (2022).
39. Madsen, M. K. *et al.* Psilocybin-induced changes in brain network integrity and segregation correlate with plasma psilocin level and psychedelic experience. *European Neuropsychopharmacology* **50**, 121–132 (2021).
40. Petri, G. *et al.* Homological scaffolds of brain functional networks. *J. R. Soc. Interface.* **11**, 20140873 (2014).
41. Lord, L.-D. *et al.* Dynamical exploration of the repertoire of brain networks at rest is modulated by psilocybin. *NeuroImage* **199**, 127–142 (2019).
42. Singleton, S. P. *et al.* Receptor-informed network control theory links LSD and psilocybin to a flattening of the brain's control energy landscape. *Nat Commun* **13**, 5812 (2022).
43. Olsen, A. S. *et al.* Psilocybin modulation of time-varying functional connectivity is associated with plasma psilocin and subjective effects. *NeuroImage* **264**, 119716 (2022).
44. Dittrich, A. The standardized psychometric assessment of altered states of consciousness (ASCs) in humans. *Pharmacopsychiatry* **31**, 80–84 (1998).
45. Mihalik, A. *et al.* Canonical Correlation Analysis and Partial Least Squares for Identifying Brain–Behavior Associations: A Tutorial and a Comparative Study. *Biological Psychiatry: Cognitive Neuroscience and Neuroimaging* **7**, 1055–1067 (2022).
46. Tagliazucchi, E. *et al.* Increased Global Functional Connectivity Correlates with LSD-Induced Ego Dissolution. *Current Biology* **26**, 1043–1050 (2016).

47. Demertzi, A. *et al.* Human consciousness is supported by dynamic complex patterns of brain signal coordination. *Science Advances* **5**, eaat7603 (2019).

48. Carhart-Harris, R. L. & Friston, K. J. REBUS and the Anarchic Brain: Toward a Unified Model of the Brain Action of Psychedelics. *Pharmacol Rev* **71**, 316–344 (2019).

49. Fukunaga, M. *et al.* Large-amplitude, spatially correlated fluctuations in BOLD fMRI signals during extended rest and early sleep stages. *Magnetic Resonance Imaging* **24**, 979–992 (2006).

50. Nilsonne, G. *et al.* Intrinsic brain connectivity after partial sleep deprivation in young and older adults: results from the Stockholm Sleepy Brain study. *Sci Rep* **7**, 9422 (2017).

51. Wong, C. W., Olafsson, V., Tal, O. & Liu, T. T. The amplitude of the resting-state fMRI global signal is related to EEG vigilance measures. *NeuroImage* **83**, 983–990 (2013).

52. Liu, X. *et al.* Subcortical evidence for a contribution of arousal to fMRI studies of brain activity. *Nat Commun* **9**, 395 (2018).

53. Mortaheb, S. *et al.* Mind blanking is a distinct mental state linked to a recurrent brain profile of globally positive connectivity during ongoing mentation. *Proceedings of the National Academy of Sciences* **119**, e2200511119 (2022).

54. Ward, A. F. & Wegner, D. M. Mind-blanking: when the mind goes away. *Front. Psychol.* **4**, (2013).

55. Andrillon, T., Burns, A., Mackay, T., Windt, J. & Tsuchiya, N. Predicting lapses of attention with sleep-like slow waves. *Nat Commun* **12**, 3657 (2021).

56. Di Plinio, S., Perrucci, M. G., Aleman, A. & Ebisch, S. J. H. I am Me: Brain systems integrate and segregate to establish a multidimensional sense of self. *NeuroImage* **205**, 116284 (2020).

57. Penny, W. D., Friston, K. J., Ashburner, J. T., Kiebel, S. J. & Nichols, T. E. *Statistical Parametric Mapping: The Analysis of Functional Brain Images*. (Elsevier, 2011).

58. Gorgolewski, K. *et al.* Nipype: A Flexible, Lightweight and Extensible Neuroimaging Data Processing Framework in Python. *Front. Neuroinform.* **5**, (2011).

59. Schaefer, A. *et al.* Local-Global Parcellation of the Human Cerebral Cortex from Intrinsic Functional Connectivity MRI. *Cerebral Cortex* **28**, 3095–3114 (2018).

60. Barttfeld, P. *et al.* Signature of consciousness in the dynamics of resting-state brain activity. *Proc. Natl. Acad. Sci. U.S.A.* **112**, 887–892 (2015).

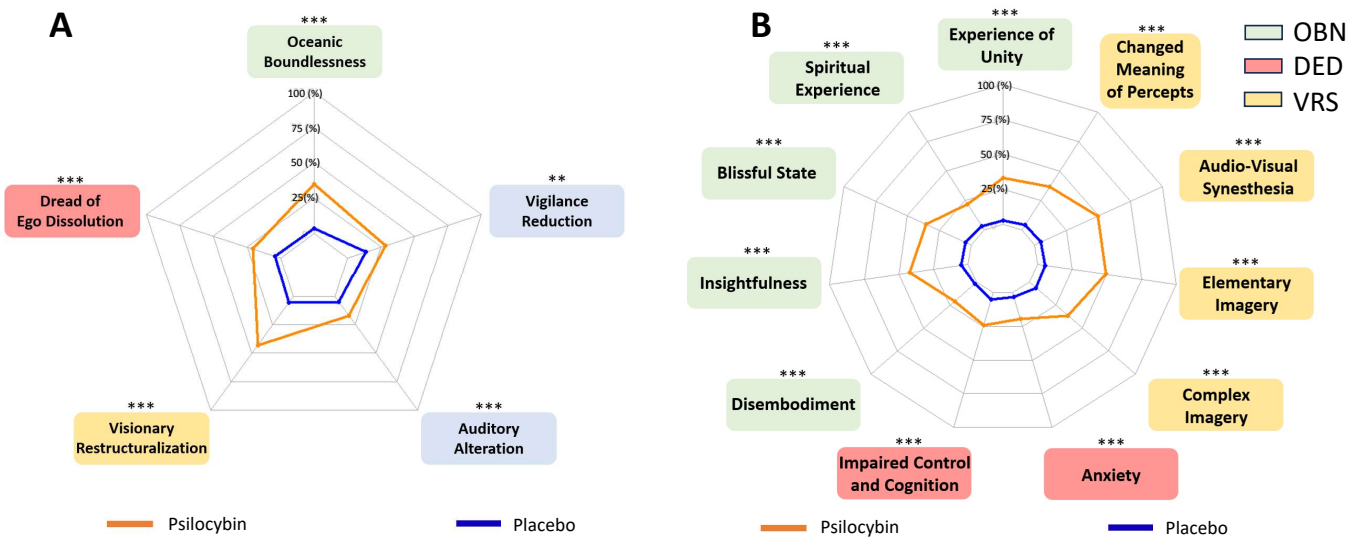

Figure 1. Substantial alterations in subjective experience were reported after psilocybin administration compared to placebo. A) The assessment of five dimensions of altered states of consciousness questionnaire (5D-ASC) showed that the administration of psilocybin significantly altered subjective experience in all dimensions. **B)** The same effect can also be observed considering the 11 factors of altered states of consciousness (11-ASC). Notes, OBN: Oceanic Boundlessness, DED: Dread of Ego Dissolution, VRS: Visionary Restructuralization. Radar plots illustrate group means for each dimension/factor.

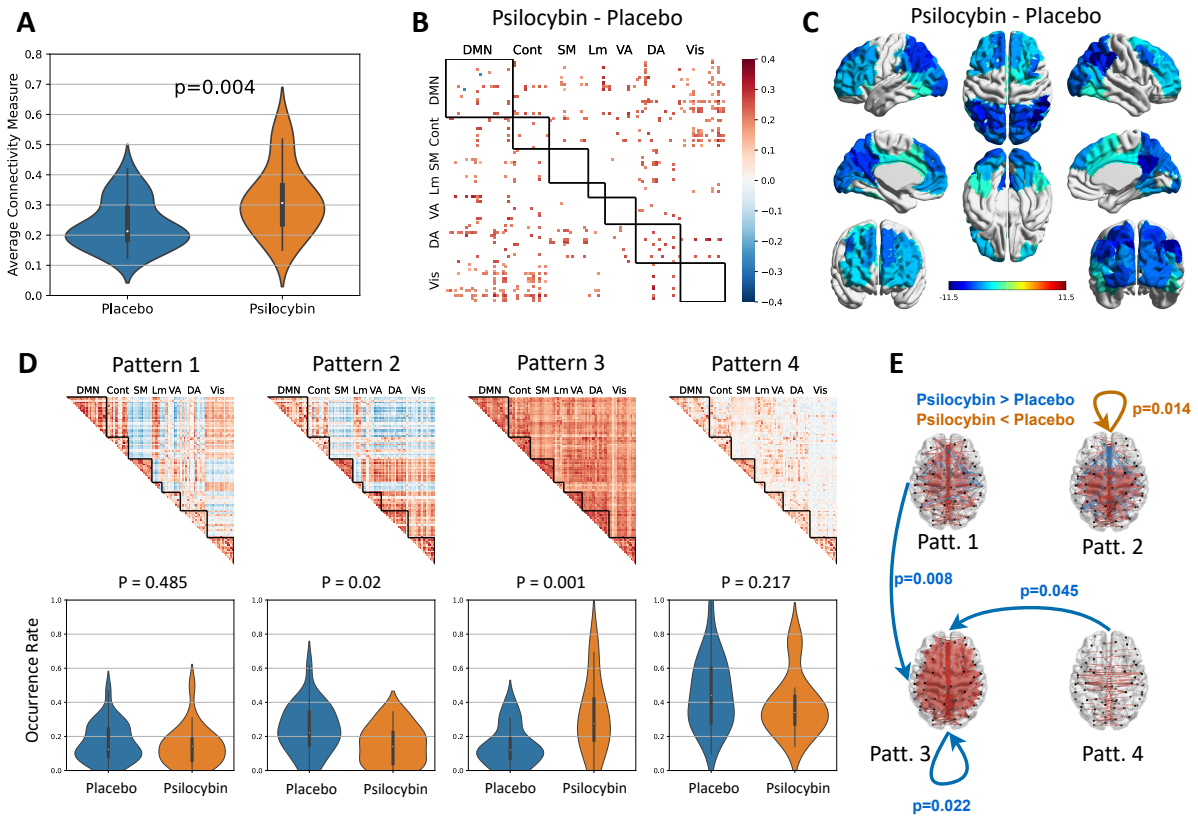

Figure 2. After psilocybin administration, there was an overall cerebral tendency to show more re-occurrence of a functional hyper-connectivity pattern. A) Averaged functional connectivity expressed as Fisher-transformed correlation values increased significantly after psilocybin administration compared to the placebo group. **B)** There were higher inter-regional connectivity values in the psilocybin group. The matrix represents the difference between the averaged connectivity matrix of the psilocybin group and that of the placebo group (contrast: psilocybin minus placebo). Only significant difference values are colored. **C)** The BOLD amplitude of posterior and anterior brain regions decreased after psilocybin administration, while the amplitude of somatomotor and limbic areas as well as the temporal regions of default more network remain unchanged. Colors are based on the difference values between the mean value of Euclidean norm of BOLD time series in the psilocybin group and the placebo group at each ROI; only significant difference values are colored. **D)** The functional connectome reconfigures in four connectivity patterns, ranging from complex inter-areal interactions (Pattern 1) to a low inter-areal

connectivity profile (Pattern 4). After psilocybin administration, there was a significant increase in the occurrence rate of the global cortex-wide positive connectivity (Pattern 3). The connectivity matrices are colored based on the connectivity value: from dark blue to dark red corresponds to connectivity values from -1 to +1. Violin plots represent the distribution of patterns' occurrence rates across participants. **E)** The transition probability from other patterns to Pattern 3 increased in the psilocybin group. Arrows indicate transitions between functional connectivity states. Blue corresponds to significantly higher transition probabilities (Wilcoxon Rank-Sum test) for the psilocybin group compared to the placebo, and orange corresponds to significantly higher transition probabilities for the placebo compared to the psilocybin group.

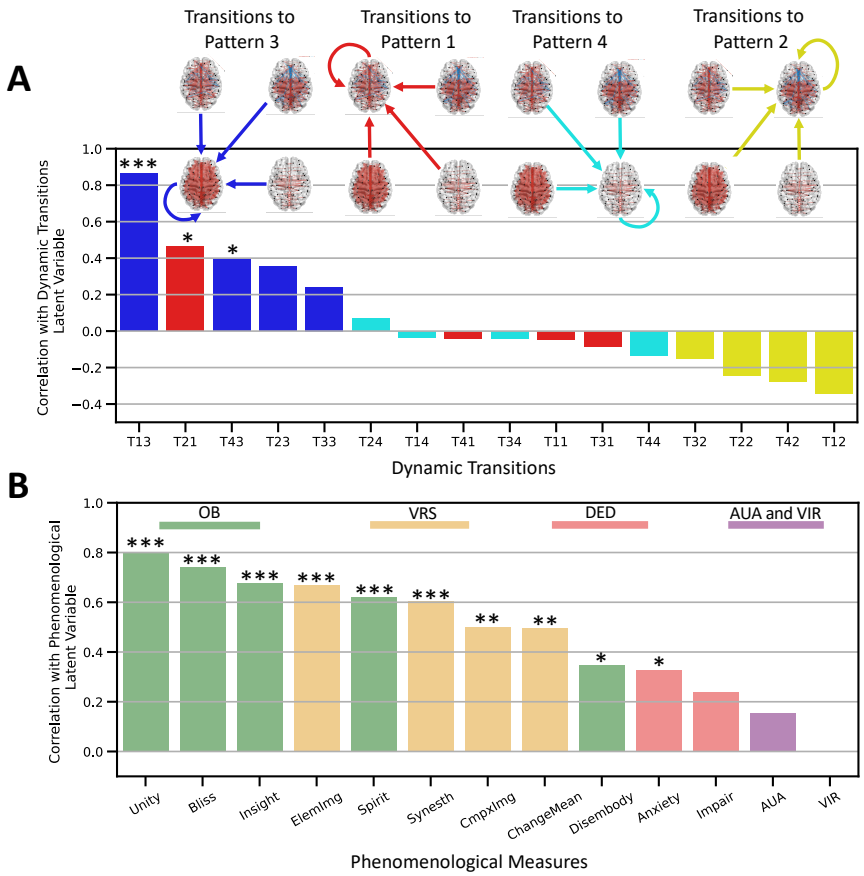

Figure 3. The neurophenomenological analysis indicated that transitions to the hyperconnected Pattern 3 were linked to the experiences of oceanic boundlessness and visionary restructuralization. A) In the neural space, the canonical correlation analysis showed that the transition probabilities to the hyperconnected pattern had the highest correlation with the first canonical vector of the space. *Notes*: Y axis represents pattern transitions, e.g T13: transition from Pattern 1 to Patten 3. **B)** In the phenomenological space, factors related to the dimension of oceanic boundlessness and visionary restructuralization showed the highest correlation with the first canonical vector of the space. Bars represent correlation values of each factor to the first canonical vector of its associated space. Asterisks represent correlation significance (*p<0.05, **p<0.01, ***p<0.001). *Notes:* Unity: experience of unity, Bliss: blissful state, Insight: insightfulness, Spirit: spiritual experience, Disembody: disembodiment, ElemImg: elementary imagery, Synesth: audio-

visual synesthesia, CmpxImg: complex imagery, ChangeMean: changed meaning of percept, Impair: Impaired control and cognition, AUA: auditory alterations, RIV: reduction of vigilance.

Table 1. There were substantial changes in subjective experience after psilocybin administration compared to placebo. Mann-Whitney U test results of comparison between 11-ASC factors of the *Psilocybin* and *Placebo* groups.

		Psilocybin (n=21)		Placebo (n=26)		Stats (MW-U test)		
		mean	**SD**	**mean**	**SD**	**U**	**rg**	**p**
5D-ASC	Oceanic Boundlessness	35.09	23.58	3.78	5.56	528.5	.936	**< 0.001**
	Dread of Ego Dissolution	20.54	17.12	3.94	8.05	494	.81	**< 0.001**
	Visionary Restructuralization	42.97	19.20	5.33	9.23	528.5	.936	**< 0.01**
	Auditory Alterations	16.99	17.18	4.69	12.97	458.5	.679	**< 0.001**
	Vigilance Reduction	28.18	20.43	13.99	16.33	400.5	.467	**< 0.001**
11-ASC	Insightfulness	42.44	29.77	4.99	7.39	508	0.861	**<0.001**
	Spiritual Experience	21.73	22.04	3.33	6.91	435	0.593	**<0.001**
	Experience of Unity	33.27	30.57	2.85	4.70	483.5	0.771	**<0.001**
	Blissful State	35.65	27.02	4.36	7.04	489	0.791	**<0.001**
	Disembodiment	20.65	25.71	1.74	1.82	434	0.59	**<0.001**
	Anxiety	19.55	22.57	3.01	4.30	430	0.575	**<0.001**
	Impaired Control and Cognition	24.29	18.35	4.77	12.51	497	0.821	**<0.001**
	Changed Meaning of Percept	36.75	29.65	4.24	8.92	495.5	0.815	**<0.001**
	Audio-Visual Synesthesia	49.54	22.82	4.94	12.99	525	0.923	**<0.001**
	Complex Imagery	36.43	25.49	6.22	12.03	528.5	0.839	**<0.001**
	Elementary Imagery	49.25	21.95	5.68	9.24	502	0.943	**<0.001**